The Association of CT-measured Cardiac Indices with Lung Involvement and Clinical Outcome in Patients with COVID-19

Vahid Eslami, MD, Alireza Abrishami, MD, MBA, Ehsan Zarei, MD, Nastaran Khalili, MD, MPH,
Zahra Baharvand, MD, MPH, Morteza Sanei-Taheri, MD

Rationale and Objectives: Cardiac indices can predict disease severity and survival in a multitude of respiratory and cardiovascular diseases. Herein, we hypothesized that CT-measured cardiac indices are correlated with severity of lung involvement and can predict survival in patients with COVID-19.

Materials and Methods: Eighty-seven patients with confirmed COVID-19 who underwent chest CT were enrolled. Cardiac indices including pulmonary artery-to-aorta ratio (PA/A), cardiothoracic ratio (CTR), epicardial adipose tissue (EAT) thickness and EAT density, inferior vena cava diameter, and transverse-to-anteroposterior trachea ratio were measured by non-enhanced CT. Logistic regression and Cox-regression analyses evaluated the association of cardiac indices with patients' outcome (death vs discharge). Linear regression analysis was used to assess the relationship between the extent of lung involvement (based on CT score) and cardiac indices.

Results: Mean ($\pm$SD) age of patients was 54.55 ($\pm$15.3) years old; 65.5% were male. Increased CTR (>0.49) was seen in 52.9% of patients and was significantly associated with increased odds and hazard of death (odds ratio [OR] = 12.5, $p = 0.005$; hazard ratio = 11.4, $p = 0.006$). PA/A >1 was present in 20.7% of patients and displayed a nonsignificant increase in odds of death (OR = 1.9, $p = 0.36$). Furthermore, extensive lung involvement was positively associated with elevated CTR and increased PA/A ($p = 0.001$).

Conclusion: CT-measured cardiac indices might have predictive value regarding survival and extent of lung involvement in hospitalized patients with COVID-19 and could possibly be used for the risk stratification of these patients and for guiding therapy decision-making. In particular, increased CTR is prevalent in patients with COVID-19 and is a powerful predictor of mortality.

Key Words: Cardiothoracic ratio; cardiac; computed tomography; COVID-19; pulmonary artery; prognosis.

INTRODUCTION

Coronavirus disease 2019 (COVID-19) is a complex infectious disease that predominantly affects the lungs (1). The burden associated with COVID-19 has already posed a serious threat to healthcare systems worldwide and will continue to exert major impact on global health until a definite vaccine or treatment is reached. With the high probability of a second wave in the near future (2), it is essential to further expand our knowledge about factors that could possibly affect survival. Early identification of patients who harbor serious illness will allow for effective triaging and prioritizing access to care for high-risk individuals.

Although most of the patients with COVID-19 develop mild type of the disease, in a minority, rapid progression of pneumonia occurs, resulting in acute respiratory distress syndrome (ARDS), multi-organ failure or even death (1,3). Initial studies have identified several factors to be associated with disease severity and survival rate. For instance, demographic factors such as older age, male sex, and presence of comorbidities such as cardiovascular diseases, as well as specific laboratory parameters are linked to unfavorable prognosis and decreased survival (4—6). However, further studies are needed to clarify other risk factors affecting patients' prognosis.

Imaging-based cardiac indices have been shown to be predictive of increased risk of morbidity and death in a variety of acute and chronic diseases. For example, an elevated cardiothoracic ratio (CTR) or increased pulmonary artery-to-aorta (PA/A) ratio is linked with unfavorable prognosis in patients with respiratory diseases (7,8); these indices might also be indicative of increased risk of cardiovascular diseases (CVD) (9,10). Other cardiac parameters such as increased epicardial adipose tissue (EAT) thickness, lower EAT density and dilated inferior vena cava (IVC) also convey prognostic information regarding major CVD and respiratory events (11−15).

Since COVID-19 is also associated with lung injury and cardiac events (16,17), these findings raise the question of whether meaningful differences also exist among survivors and non-survivors of COVID-19 in terms of cardiac parameters and pulmonary vasculature. In this study, we hypothesized that CT-based cardiac indices are correlated with severity of pulmonary involvement and can predict the prognosis and outcome of patients with COVID-19.

METHODS

Ethics Approval

The ethical review board of our institution approved the study. Written informed consent was obtained from all individuals prior to being enrolled in the study. All investigations were conducted in accordance with the 1964 Declaration of Helsinki and its later amendments.

Study Design and Patient Population

This single-center prospective study was conducted on patients with confirmed diagnosis of COVID-19 who were admitted to our academic tertiary hospital from February 20, 2020 to April 10, 2020. Inclusion criteria were as follows: (1) Confirmed diagnosis of COVID-19 through real-time reverse transcriptase polymerase chain reaction (RT-PCR) assay with samples obtained from nasopharyngeal swab; (2) chest CT imaging suggestive for COVID-19 pneumonia; and (3) age older than 18 years. Exclusion criteria were as follows: (1) positive history of pulmonary emboli; (2) history of oxygen-dependent COPD; (3) being treated only as outpatient; and (4) poor or suboptimal image quality due to severe cardiac motion artifact. On admission, patients' information regarding demographic data, past medical history, laboratory tests and presenting signs and symptoms was obtained through a predesigned questionnaire filled by an independent investigator. Furthermore, the imaging findings of patients' initial chest CT were recorded. All patients were followed until one of the study endpoints (defined as either death or complete recovery and discharge) were reached.

Laboratory Procedures

RT-PCR for SARS-CoV-2 (DAAN gene Co Ltd device) was performed on the nasopharyngeal swab specimen of all patients. Laboratory tests including biochemistry, complete blood count (CBC), and indices such as neutrophil-to-lymphocyte ratio (NLR) and platelet-to-lymphocyte ratio (PLR), and inflammatory markers such as C-reactive protein (CRP), creatine phosphokinase (CPK), and lactase dehydrogenase level (LDH) were recorded at admission. CRP levels were measured using the Rondox essay kit with immunoturbidimetric techniques. For the assessment of CBC, NLR and PLR, venous blood samples were collected in potassium ethylenediaminetetraacetic acid tubes (dipotassium EDTA tubes) and the Sysmex-XE 2000i automated blood cell analyzer (Sysmex, Kobe, Japan) was used for measurement within an hour. This is the standard duration time for our laboratory, since it prevents EDTA-induced swelling.

Chest CT Imaging

As part of national COVID-19 guidelines, all clinically suspected patients underwent low-dose non–enhanced chest CT at admission (18). In patients with more than one CT, only the initial CT was evaluated. CT was performed for every patient using a 64-slice scanner (Siemens sensation; Siemens Healthineers, Erlangen, Germany) in supine position during end-inspiration. A low–dose CT protocol with the following scanning parameters was applied: Gantry rotation time of 0.5 seconds, 0.625 mm × 64-detector array, pitch of 1.4, table speed of 45.2 mm/rotation, 20 mAs, 120 kVp, and a 300 × 300 matrix. CARE Dose4D and CARE kV scanning parameters were off. A 1 mm slice thickness and 1mm reconstruction interval was used for sagittal and coronal image reconstruction. After each CT, passive air ventilation was performed for at least 30 minutes and machine surfaces were disinfected with ethanol and didecyldimethylammonium chloride (DDAC).

DICOM data were transferred onto a picture archiving and communicating system (PACS). Then, two expert radiologists with 9 and 18 years of experience independently interpreted the images and a final decision was reached by consensus. Both radiologists were blinded to laboratory data, clinical features, and patients' diagnosis. In case of disagreement, the opinion of a third radiologist was used. All CT images were viewed in axial, sagittal and coronal planes. Predominant pattern of involvement was classified as ground-glass opacification, consolidation, reticular or mixed. In addition, axial, and anteroposterior lesion distribution was also recorded. Furthermore, the presence of other imaging features such as pleural and pericardial effusion, crazy-paving pattern, reversed halo sign, airway thickening, vessel dilatation (defined as vessel diameter larger than expected for the point within the vascular tree, characterized by 1) vessel diameter larger than that in adjacent portions of nondiseased lung, (2) vessel diameter larger than that in comparable regions of nondiseased contralateral lung, or (3) focal dilation or non-tapering of vessels as they course toward the lung periphery), airway dilatation, air bronchogram, and lymph node with a short-axis diameter of larger than 1 cm was

assessed. For evaluation of zonal involvement, three zones were defined as follows: (1) Upper zone: area above the carina region; (2) middle zone: area between the carina and inferior pulmonary vein; and (3) lower zone: area below the inferior pulmonary vein. The percentage of lung involvement was scored using the following system: 0: no involvement, 1: <25%, 2: 26%-50%, 3: 51%-75% and 4: >75%. Zonal scores of both lungs were summed up to calculate upper, middle, and lower zone score (maximum score of each zone = 8). Total lung score was calculated by summing scores of all of the three zones (maximum score = 24).

All dimensions of cardiac indices were derived from low-dose non-enhanced multidetector chest CT scan. Cardiothoracic ratio was defined as the greatest transverse cardiac diameter from outer to outer myocardium divided by the greatest transverse thoracic diameter from inner to inner chest wall on axial images, usually at the level of the diaphragmatic apex (Fig. 1A) (19,20). CTR ≥ 0.49 was considered as an indicator of cardiac enlargement (20). PA/A was calculated as the ratio of the PA measured at the level of the PA bifurcation to the ascending aortic diameter measured from the same CT slice using mediastinal windows (Fig. 1B). PA enlargement was defined as PA/A>1. The average anteroposterior and

(a)

(b)

Figure 1. (A and B). Axial images of chest computed tomography (CT) showing measurement of cardiac indices. (A) *CT-derived cardiothoracic ratio:* The short arrow depicts the greatest transverse cardiac diameter and the longer arrow indicates the greatest transverse thoracic diameter. The thoracic diameter would normally be taken few centimeters caudal to this image; at the level of the dome of the hemidiaphragm (It has been included at this level only to simulate the measurement and to complete the figure). (B) *CT-derived pulmonary artery-to-aorta ratio (PA/A).*

transverse diameters of IVC were measured at the level of the right diaphragmatic crus. Epicardial fat was defined as the adipose tissue between the visceral epicardium to the outside of the myocardium. EAT thickness (mm) was measured on the right ventricular (RV) anterior free wall and perpendicular to the surface of the heart on short-axis views of a regular workstation. EAT thickness measurements were made at three levels including inferior, middle, and superior, corresponding to measurements at the 25%, 50%, and 75% level of the RV wall, respectively. Of these three measurements, the mean value was considered as EAT thickness and was included in the analysis. EAT density was also measured at these three levels (Fig. 2A & B). The area of interest was defined by the manual delineation of the pericardium and the density was calculated in a workstation by specific software. The mean density of the adipose tissue in these three levels was considered as EAT density. Transverse and anteroposterior tracheal dimensions were measured at right below the notch of the sternal manubrium.
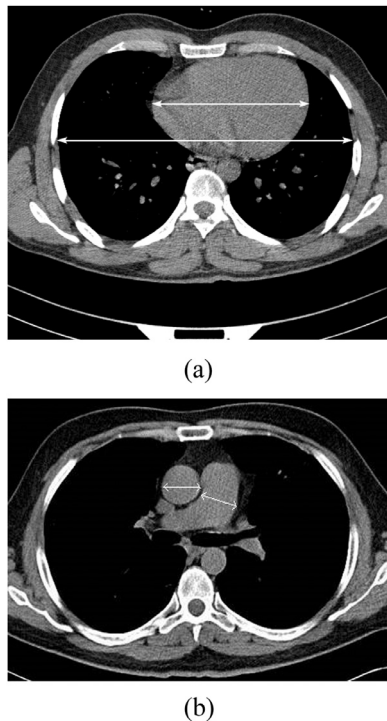
Statistical Analysis

Normal continuous variables are represented as mean ± SD and skewed continuous variables are expressed as median (quartile 1−quartile 3). Categorical data are reported as frequency (percentage). Independent *t* test and Mann-Whitney *U* test were used for comparison of normal and skewed data between death and discharged patients. Chi-square test was used for comparison of categorical variables. Logistic regression and Cox-regression for survival analyses were applied for evaluating the effect of cardiac indices on patient's outcome (death vs discharge). In the Cox model, "outcome" was defined as "death or discharge" and "length of hospitalization" was considered as "time to outcome". Also, the association between lung involvement and cardiac size variables was tested by linear regression models, in which cardiac factors were considered as dependent variables. Both logistic and linear regression analyses were adjusted for age, sex, and presence of any comorbidities (including hypertension, ischemic heart disease, chronic kidney disease, chronic liver disease, congestive heart failure, diabetes mellitus, non-oxygen dependent COPD, asthma). A *p*-value <0.05 was considered statistically significant. All statistical analysis was performed by STATA 14 and SPSS version 24 (IBM Inc., Chicago, IL).

RESULTS

Patients' Demographic, Clinical, and Imaging Features

Baseline demographic, clinical, and imaging characteristics of patients are shown in Table 1. Eighty-seven patients were included in the final analysis. Mean age of patients was 54.55 ± 15.3 years old; 57 (65.5%) were male. The distribution of age ($p = 0.99$) and sex ($p = 0.22$) was equal between discharged and deceased patients. On follow-up, 13 of 87 patients (14.9%) died and the rest were discharged. Cough

Figure 2. (A and B). EAT thickness and density measurements were made at three levels (A) Corresponding to measurements at 25%, 50%, and 75% level of the RV wall. Of these three measurements, (B) the mean value was considered as EAT thickness and was included in the analysis. EAT density was also measured at these three levels. The area of interest was defined by manual delineation of the pericardium and then density was calculated in a workstation by specific software. (Color version of figure is available online.)

(69%), fever (64.4%), and dyspnea (62.1%) were the most common clinical manifestations; diarrhea (9.5%) and abdominal pain (11.5%) were the least common. None of the reported clinical symptoms differed significantly between the two groups ($p > 0.05$). The median length of hospital stay was significantly higher in deceased patients (15 vs 9 days, $p = 0.003$). There was no significant difference in the presence of any major comorbidity across the deceased patients and those who survived. Evaluation of laboratory finding showed that median NLR ($p = 0.04$), and LDH ($p = 0.002$) were significantly more increased in deceased patients, whereas lymphocyte-to-CRP ratio was significantly less in these patients ($p = 0.01$).

As shown in Table 1, the extent of total lung involvement, as well as involvement of each of the individual zones (upper, middle, and lower zone) was significantly higher in deceased patients compared with discharged patients ($p < 0.01$). A significant difference existed in terms of anteroposterior distribution of lesions between the two groups ($p = 0.04$). Overall, GGO was the most frequent involvement pattern followed by consolidation. Regarding other imaging findings, vessel dilatation existed in all of the patients who died while only 62.2% of discharged patients were positive for this finding ($p = 0.007$). In terms of cardiac indices, a significantly higher CTR was observed in patients who died ($p = 0.03$); however, EAT density was significantly lower in these patients ($p = 0.04$).

Hazard Ratio and Odds Ratio of Death Contributed to Cardiac Indices

The probability of death in patients with PA/A > 1 was 22.2% compared with 13.0% in those with a PA/A ≤ 1. Furthermore, elevated CTR (≥0.49) was associated with more than four-fold increase (23.9% vs 4.9%) in the probability of death as compared with lower CTR. Adjusted analysis revealed that the odds of death was significantly higher in patients with higher CTR (odds ratio [OR] = 12.5, $p = 0.005$). Elevated PA/A also increased the odds of death;

however this association was not significant (OR = 1.9, $p = 0.36$) (Table 2).

By considering "death" as the event and "duration of hospitalization" as the event time in Cox regression analysis, the effect of PA/A and CTR were tested on the hazard rate of death in COVID-19 patients. In adjusted cox models, elevated CTR significantly increased the hazard of death (hazard ratio [HR] = 11.4, $p = 0.006$). This association was not significant for PA/A (HR = 1.35, $p = 0.63$). Figure 3 indicates the higher risk of death with higher level of PA/A and CTR during the follow-up period. Proportionality of hazards in cox regression analysis was evaluated and confirmed, as presented in the appendix.

Association Between Cardiac Indices and Lung Involvement Scores

The extent of lung involvement in the upper ($\beta = 0.02$, $p = 0.006$), middle ($\beta = 0.03$, $p < 0.001$), and lower zone ($\beta = 0.02$, $p = 0.004$) was positively related to PA/A>1 (Fig. 4); a significant association was also observed between higher total score and increased PA/A ($\beta = 0.01$, $p = 0.001$). Similarly, there was a significant correlation between greater zonal and total lung scores and elevated CTR (Table 3).

DISCUSSION

Integration of imaging findings into standard clinical practice is an asset for patient management in any disease. Although many studies have addressed the extent of lung involvement on CT as a predictor for clinical severity and disease burden in patients with COVID-19 (21,22), the prognostic value of CT-measured cardiac indices has not yet received enough attention. Our study revealed that increased CTR is prevalent in hospitalized patients with COVID-19 and is a powerful predictor of mortality in these patients. Pulmonary enlargement, defined as PA/A >1, was also associated with a nonsignificant increase in the odds of COVID-19-related death. In

TABLE 1. Patient's Baseline Demographic Characteristics, Clinical Data and Imaging Findings

	Total $N = 87$	Discharged $N = 74$ (85.1%)	Deceased $N = 13$ (14.9%)	p-Value
Age (years)	54.55 ± 15.30	54.55 ± 15.63	54.54 ± 13.85	0.99
Sex				0.20
Male	57 (65.5)	46 (62.2)	11 (84.6)	
Female	30 (34.5)	28 (37.8)	2 (15.4)	
Duration of hospitalization (days)	10 (5−15)	9 (4.8−13.3)	15 (11−20.5)	0.003
SpO$_2$ (%)	90 (88−93)	91 (88−93)	88 (85.5−90.8)	0.10
Comorbidity factors				
Asthma/COPD[a]	7 (8.0)	6 (8.1)	1 (7.7)	0.99
Diabetes mellitus	15 (17.2)	14 (18.9)	1 (7.7)	0.45
Ischemic heart disease/CHF	15 (17.2)	11 (14.9)	4 (30.8)	0.23
Hypertension	20 (23.0)	18 (24.3)	2 (15.4)	0.72
Chronic kidney disease	19 (21.8)	13 (17.8)	6 (46.2)	0.03
Chronic liver disease	1 (1.4)	1 (1.3)	0 (0)	0.99
Presence of any comorbidity[b]	49 (56.3)	40 (54.1)	9 (69.2)	0.38
Laboratory findings				
Leukocyte (× 10^9/L)	5.3 (4.1−7.2)	5.3 (4.1−7.0)	6.4 (4.0−8.6)	0.37
Platelet (× 10^9/L)	194 (140−254)	200 (144−263)	171 (128.5− 208)	0.12
Neutrophil (× 10^9/L)	3.8 (2.9−5.2)	3.7 (2.9−5.2)	5.2 (2.8−7.3)	0.17
Lymphocyte (× 10^9/L)	1.1 (0.9−1.6)	1.2 (0.9−1.6)	1.0 (0.7−1.4)	0.15
Neutrophil-to-lymphocyte ratio	3.1 (2.3−4.2)	3.0 (2.2−4.0)	3.8 (2.5−11.2)	0.04
Platelet-to-lymphocyte ratio	1.6 (1.2−2.2)	1.6 (1.2−2.2)	2.1 (1.1−2.7)	0.36
Troponin (× 10^3)	2 (1−7)	2 (1−5.5)	2.5 (1.3−7.5)	0.28
C-reactive protein (mg/dL)	36.5 (15−50)	36 (10.8− 47.3)	49.0 (33−57)	0.054
Creatine phosphokinase (IU/l)	141 (62−389)	141 (61−391)	103 (60−438)	0.90
Lactate dehydrogenase (IU/l)	420 (332−556)	385 (311−493)	578 (469−1316)	0.002
Lymphocyte-to-CRP ratio	0.04 (0.02−0.08)	0.04 (0.02−0.1)	0.02 (0.01−0.04)	0.01
Imaging findings				
Lung involvement scores				
Upper zone score	2 (1−4)	2 (1−3)	3 (2−5)	0.02
Middle zone score	3 (2−6)	3 (2−5)	6 (5−6.5)	<0.001
Lower zone score	4 (2−6)	3.5 (2−6)	7 (4.5−8)	0.001
Total score	9 (5−15)	8 (5−14)	16 (12.5−18.5)	0.001
Pattern of involvement				0.22
Ground glass opacity	58 (66.7)	51 (68.9)	7 (53.8)	
Consolidation	14 (16.1)	10 (13.5)	4 (30.8)	
Reticular	7 (8.0)	7 (9.5)	0 (0)	
Mixed	8 (9.2)	6 (8.1)	2 (15.4)	
Lesion distribution extension				0.20
Unilateral	12 (13.8)	12 (16.2)	0 (0)	
Bilateral	75 (86.2)	62 (83.8.7)	13 (100)	
Axial				0.25
Peripheral	66 (75.9)	58 (78.4)	8 (61.5)	
Central	6 (6.9)	5 (6.8)	1 (7.7)	
Both	15 (17.2)	1 (14.9)	4 (30.8)	
Anteroposterior				
Posterior	59 (67.8)	54 (73.0)	5 (38.5)	0.04
Anterior	6 (6.9)	4 (5.4)	2 (15.4)	
Lateral	2 (2.3)	1 (1.4)	1 (7.7)	
Nonspecific	20 (23.0)	15 (20.3)	5 (38.5)	
Other abnormal findings				
Airway thickening	68 (78.2)	56 (75.7)	12 (92.3)	0.28
Crazy-paving	12 (13.8)	10 (13.5)	2 (15.4)	0.99
Reversed-halo sign	1 (1.4)	1 (100)	0 (0)	0.99
Lymphadenopathy[c]	4 (4.6)	3 (4.1)	1 (7.7)	0.48
Dilated vessel	59 (67.8)	46 (62.2)	13 (100)	0.007

(continued)

TABLE 1. (Continued)

	Total N = 87	Discharged N = 74 (85.1%)	Deceased N = 13 (14.9%)	p-Value
Airway dilatation	37 (42.5)	29 (39.2)	8 (61.5)	0.22
Air bronchogram	30 (34.5)	23 (31.1)	7 (53.8)	0.13
Septal thickening	12 (13.8)	10 (13.5)	2 (15.4)	0.99
Cyst	11 (12.6)	11 (14.9)	0 (0)	0.20
Pleural effusion	14 (16.1)	11 (14.9)	3 (23.1)	0.68
Pericardial effusion	15 (17.2)	12 (16.2)	3 (23.1)	0.69
Cardiac indices				
Pulmonary artery (mm)	29.43 ± 5.01	29.15 ± 4.98	31.08 ± 5.04	0.20
Aorta (mm)	33.77 ± 4.49	33.74 ± 4.35	33.92 ± 5.42	0.89
Pulmonary artery/aorta	0.88 ± 0.15	0.87 ± 0.14	0.93 ± 0.15	0.19
T/AP inferior vena cava	1.11 ± 0.23	1.11 ± 0.25	1.10 ± 0.21	0.85
Long /Short axis	1.5 (1.4−1.69)	1.5 (1.4−1.7)	1.6 (1.4−1.7)	0.48
Cardiothoracic ratio	0.50 ± 0.06	0.50 ± 0.07	0.53 ± 0.05	0.033
T/AP trachea	0.95 ± 0.18	0.94 ± 0.17	0.98 ± 0.25	0.51
Epicardial adipose tissue thickness (mm)	6.1 (4.7−8.0)	6.0 (4.7−7.9)	7.8 (4.8−9.8)	0.22
Epicardial adipose tissue density (Hounsfield Unit)	−89 (−106−−75)	−86 (−101−−75)	−103 (−119−−86)	0.044

CHF, congestive heart failure; COPD, chronic obstructive pulmonary disease; T/AP, transverse/anteroposterior.

a This included non-oxygen dependent COPD patients.

b The presence of at least one comorbidity.

c Defined as a lymph node with a short-axis diameter > 10 mmNote: Data are represented as mean ± SD, median (Q1−Q3), and frequency (percent).Mean and median differences were tested using independent T-test and Mann-Whitney U test, respectively. The distribution of categorical data was compared by chi-square test (with exact p-value).

addition, we showed that more extensive lung involvement on CT is positively related with increased CTR and PA/A.

Evaluation of cardiovascular parameters has recently gained attention in predicting the survival of patients with COVID-19. A recent study conducted in New York on 105 patients with SARS-CoV-2 infection showed that right ventricular dilatation is strongly associated with in-hospital mortality. They also noted that right ventricular dilation is present in 31% of hospitalized patients. A focused, time-efficient echocardiography protocol was used to measure ventricular size in the mentioned study (23). In line with this finding, another study performed in Wuhan reported that right ventricular longitudinal strain on echocardiography is an independent determinant of outcome in patients with COVID-19. Of note, they found that pulmonary artery systolic pressure was higher in patients

who had not survived (24). We also observed that an increased CTR exists in more than half of patients who are hospitalized and in 76% of patients who eventually die and is significantly associated with poor disease outcome. Our results also demonstrated a nonsignificant increase in the odds of death in patients with PA/A > 1, which has previously been suggested as a possible marker of pulmonary hypertension (PH) (25). Nevertheless, a recent study on 45 patients with COVID-19 infection showed that increased PA at admission was associated with death while increased PA/A was not linked with an unfavorable outcome (26).

EAT thickness and density, as well as IVC dimensions, have been previously proposed to be useful predictive markers of adverse cardiac events and survival (11,13−15). In patients with COVID-19, acute cardiac injury is a frequent

TABLE 2. The Hazard and Odds of Death-related to PA/A and Cardiothoracic Ratio in Patients with COVID-19

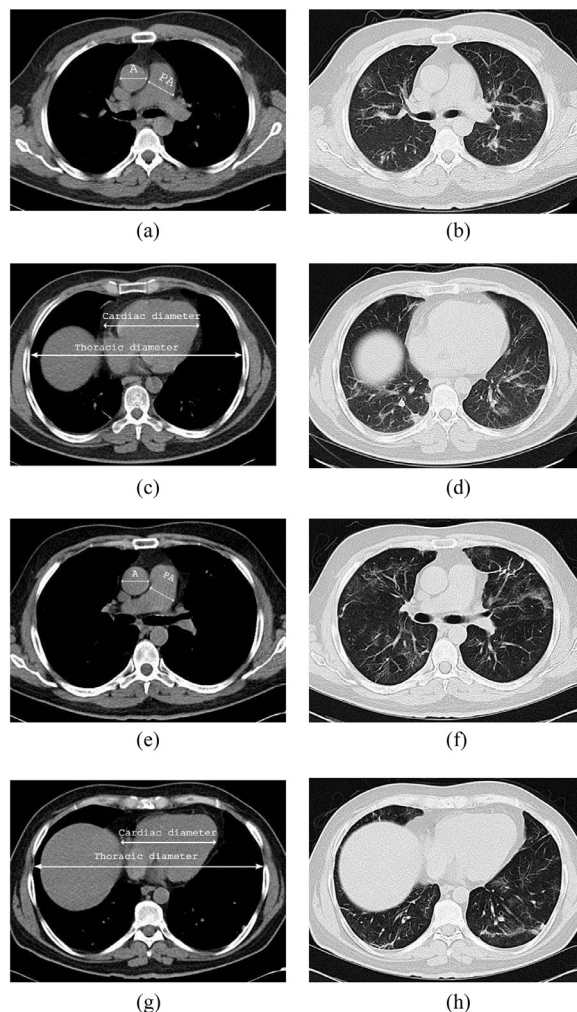|	Total (N = 87)	Discharged (N = 74)	Death (N = 13)	Logistic Model[a]		Cox Model[a]	
				OR (95% CI)	p-value	HR (95% CI)	p-value
PA/Aorta							
>1.0	18 (20.7%)	14 (18.9%)	4 (30.7%)	1.90 (0.47−7.62)	0.36	1.35 (0.41−4.44)	0.63
≤1.0	69 (79.3%)	60 (81.1%)	9 (69.2%)				
CTR							
≥0.49	46	35 (47.2%)	11 (84.6%)	12.49 (2.10−47.22)	0.005	11.35 (2.04−36.11)	0.006
<0.49	41	39 (52.7%)	2 (15.4%)				

CI, confidence interval; CTR, cardiothoracic ratio; HR, hazard ratio; OR, odds ratio; PA/A, pulmonary artery-to-aorta ratio.

a Adjusted for age, sex, and comorbidity status.

(a)

(b)
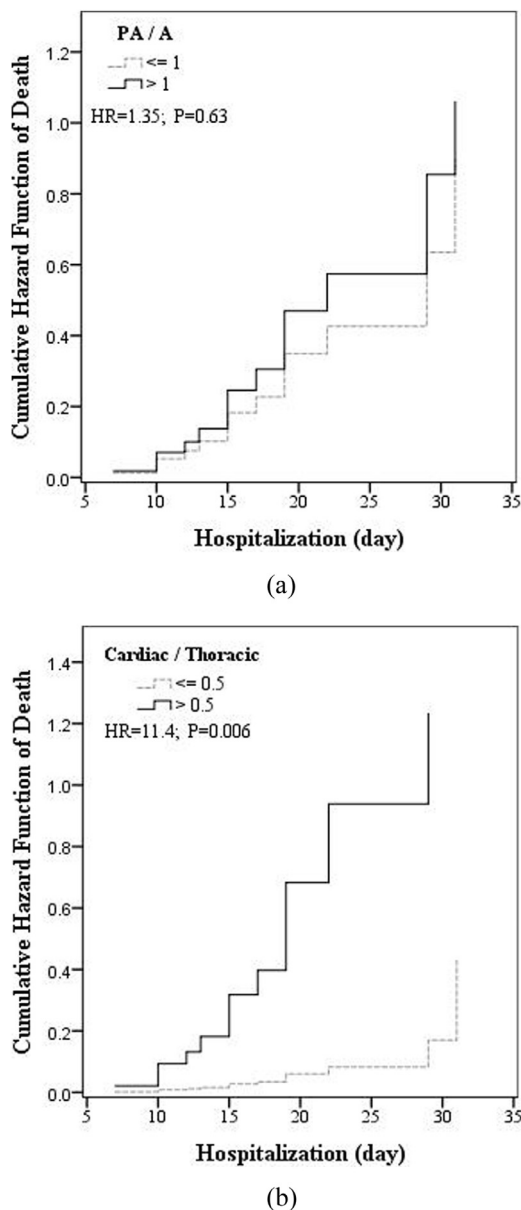
Figure 3. (A and B). Cumulative hazard function of death in patients according to (A) pulmonary artery-to-aorta ratio and (B) cardiothoracic ratio. Outcome was defined as *death* or *discharge* and *length of hospitalization* was considered as time to outcome in the cox regression analysis. (Color version of figure is available online.)

Figure 4. (A−H). A 45-year-old man presented with dry cough, dyspnea (SpO$_2$: 88%) and abdominal pain without history of any comorbidity. Computed tomography (CT) images (A and B) obtained 5 days after the onset of symptoms show patchy ground-glass opacity in both lungs with increased pulmonary artery-to-aorta ratio (1.07) and (C and D) normal cardiothoracic ratio (0.46). CT images (E and F) obtained 28 days after symptoms onset show evolution of the area of ground glass opacities with reticular pattern and normal pulmonary artery-to-aorta ratio (1.00) and (G and H) normal cardiothoracic ratio (0.43). The patient was discharged after 26 days.

complication, since these patients are exposed to an increased risk of acute coronary artery disease, cardiogenic shock, and heart failure (16,27,28). Moreover, it has been shown that the occurrence of acute cardiac events increases the risk of COVID-19-related death (29). Despite this, we were not able to show an increased chance of death in patients with a dilated IVC, increased EAT thickness, or lower EAT density. However, we observed that the mean EAT density was markedly lower in deceased patients compared with the survivors; although this significant difference was not seen across the two groups in terms of IVC dimension or EAT thickness.

As previously discussed, the extent of lung involvement on CT is shown to be related with clinical severity and prognosis of patients with COVID-19 (21,22). Our results confirmed this finding, showing that the amount of total lung involvement was significantly higher in deceased patients compared with those who were discharged. Also, in those who died, a significantly greater extent of involvement was seen in all three zones (upper, middle, and lower). In this study, we also assessed the relation between degrees of lung involvement with CT-measured cardiac indices. We found a positive correlation between higher lung involvement CT scores with elevated CTR (≥0.49) and increased PA/A (>1). As previously mentioned, studies have demonstrated an association between increased CTR and risk of adverse cardiovascular

TABLE 3. Adjusted Linear Regression Analysis[a] Showing the Relationship Between Cardiac Indices and Lung Involvement Scores in COVID-19 Patients

Dependents	Upper Zone		Middle Zone		Lower Zone		Total Zone	
	β (SE)	p-value	β (SE)	p-value	β (SE)	p-value	β (SE)	p-value
PA/A	0.023 (0.01)	0.006	0.026 (0.007)	<0.001	0.02 (0.006)	0.004	0.01 (0.002)	0.001
CTR	0.007 (0.003)	0.026	0.008 (0.003)	0.002	0.009 (0.002)	<0.001	0.003 (0.001)	0.001
T/AP IVC	−0.006 (0.01)	0.64	−0.007 (0.01)	0.54	−0.001 (0.01)	0.93	0.001 (0.004)	0.92
Long/Short axis	0.18 (0.09)	0.039	0.18 (0.08)	0.025	0.11 (0.07)	0.11	0.06 (0.03)	0.036
T/AP trachea	0.009 (0.01)	0.40	0.014 (0.01)	0.13	0.013 (0.01)	0.10	0.005 (0.003)	0.14
EAT thickness	0.15 (0.13)	0.24	0.14 (0.11)	0.22	0.04 (0.10)	0.67	0.04 (0.04)	0.33
EAT density	2.37 (1.14)	0.040	1.31 (1.12)	0.25	1.13 (0.99)	0.26	0.58 (0.40)	0.14

CTR, cardiothoracic ratio; EAT, epicardial adipose tissue; IVC, inferior vena cava; PA/A, pulmonary artery-to-aorta ratio; T/AP, transverse/anteroposterior.

a Analysis was adjusted for age, sex and comorbidities.

events(10), thus, an elevated CTR subsequent to extensive lung involvement could be the possible reason that attributed to more severe form of disease and consequently, higher risk of death in our patients. Furthermore, as already known, acute lung injury is an established cause of PH and right ventricular dysfunction (30). This possibly justifies the observed association between more extensive lung involvement and elevated PA/A ratio in our study. In line with our results, Spagnolo et al. also showed that PA/A ratio significantly increased subsequent to COVID-19 infection and was significantly correlated with the extent of pneumonia (26).

As a secondary objective, we also evaluated the CT imaging features of all patients. As in other reports, the results of our study showed that bilateral GGO and consolidation are the predominant involvement patterns (31). We also observed posterior distribution of lesions mainly in the periphery of lungs, which is in agreement with that of other previous studies (32). Airway thickening was a prevalent finding, observed in more than 90% of deceased patients. In addition, we found that vessel dilatation was significantly more prevalent in deceased patients. Interestingly, another study reported prognostic value of vessel dilatation, suggesting that this finding is related to severe forms of COVID-19 (33).

In our country, from the beginning of the COVID-19 pandemic, low-dose chest CT was performed at admission for all patients who presented with high clinical suspicion of COVID-19 as part of their routine work-up. This extensive use of CT provided an advantage for simultaneous identification of unknown possible prognostic markers of COVID-19 such as cardiac indices. Although low-dose chest CT might not be the best modality for measuring cardiac indices, compared to other techniques, it is safer, rapid, and readily available while also having acceptable performance (8,19,34). For instance, right heart catheterization, which is the golden standard test for the diagnosis of PH (35), is costly and aggressive, contributing to serious adverse events such as pneumothorax, arrhythmias and even death in unstable patients (36,37). Also, despite the fact that chest X-ray is widely utilized for the measurement of CTR, it is difficult and suboptimal to perform plain chest radiography for most hospitalized patients

with COVID-19 since it requires upright position and unlike chest CT, it does not provide further diagnostic and prognostic value in the setting of COVID-19. Reports from previous studies indicate that routine non-cardiac CT is also efficient for the measurement of CTR and does not display statistically significant difference as compared with radiography (19,38). A recent study showed that CTR measured by routine non-gated CT is strongly correlated with that of chest X-ray (r = 0.802) (20). Although other methods such as ECG-gated CT scan might be more accurate for obtaining estimates of cardiomegaly, they are time-consuming and often require specific protocols or software (39). A recent study suggested that, due to the risk of decontamination, echocardiography should not be routinely performed in patients with typical signs of COVID-19 disease and instead modalities such as CT were recommended as safer alternatives for cardiac imaging (40). Thus, in the setting of COVID-19, routine chest CT could be considered as an appropriate and practical tool for the primary assessment of cardiac indices and act as a gatekeeper before performing further evaluations. In addition to providing prognostic information, the early suspicion of possible conditions such as cardiomegaly and pulmonary hypertension at admission could provide guidance for wisely treatment of patients with COVID-19.

Our study had some limitations. First, the sample size was relatively small. Second, as part of national COVID-19 guidelines, non-contrast non-gated chest CT was used for all patients. This resulted in decreased accuracy of some measurements, particularly in obese patients. Another point which should be considered is that the effect of cardiac motion and respiratory changes was not assessed in our study, which might possibly influence the measurement of indices such as EAT and IVC. We also acknowledge that patients' body mass index is an important prognostic factor that might affect results; however due to some limitations, we were unable to measure patients' body mass index at admission.

In conclusion, the results of our study showed that increased CTR is prevalent in patients with COVID-19 and is a powerful predictor of mortality in hospitalized patients. We also observed that an elevated PA/A ratio is associated

with a nonsignificant increase in odds of death and could be used as a possible prognostic marker of COVID–19. Furthermore, higher lung involvement scores were related with elevated CTR and PA/A on CT. Overall, the results of our study suggest that primary assessment of cardiac indices on routine CT might convey useful prognostic information regarding the survival and extent of lung involvement in hospitalized patients with COVID-19 and could be beneficial in the risk stratification of patients as well as guiding therapy decision-making.

FUNDING

DECLARATIONS OF INTEREST

None.

REFERENCES

1. Huang C, Wang Y, Li X, et al. Clinical features of patients infected with 2019 novel coronavirus in Wuhan, China. The Lancet 2020; 395 (10223):497–506.
2. Zhu N, Zhang D, Wang W, et al. A novel coronavirus from patients with pneumonia in China, 2019. N Engl J Med 2020; 382(8):727–733. doi:10.1056/NEJMoa2001017. 2020/02//.
3. Guan WJ, Ni ZY, Hu Y, et al. Clinical characteristics of coronavirus disease 2019 in China. N Engl J Med 2020. doi:10.1056/NEJMoa2002032.
4. Wu JT, Leung K, Bushman M, et al. Estimating clinical severity of COVID-19 from the transmission dynamics in Wuhan, China Nat Med 2020; 26 (4):506–510. doi:10.1038/s41591-020-0822-7.
5. Tan L, Wang Q, Zhang D, et al. Lymphopenia predicts disease severity of COVID-19: a descriptive and predictive study. Signal Transduct Targeted Ther 2020; 5(1):33. doi:10.1038/s41392-020-0148-4. 2020/03/27.
6. Terpos E, Ntanasis-Stathopoulos I, Elalamy I, et al. Hematological findings and complications of COVID-19. Am J Hematol 2020. doi:10.1002/ajh.25829. 2020/04//.
7. Zouk AN, Gulati S, Xing D, et al. Pulmonary artery enlargement is associated with pulmonary hypertension and decreased survival in severe cystic fibrosis: a cohort study. PLoS One 2020; 15(2): e0229173. doi:10.1371/journal.pone.0229173.
8. Wells JM, Morrison JB, Bhatt SP, et al. Pulmonary artery enlargement is associated with cardiac injury during severe exacerbations of COPD. Chest 2016; 149(5):1197–1204.
9. Ogata H, Kumasawa J, Fukuma S, et al. The cardiothoracic ratio and all-cause and cardiovascular disease mortality in patients undergoing maintenance hemodialysis: results of the MBD-5D study. Clin Exp Nephrol 2017; 21(5):797–806. doi:10.1007/s10157-017-1380-2. 2017/10/01.
10. Okute Y, Shoji T, Hayashi T, et al. Cardiothoracic ratio as a predictor of cardiovascular events in a cohort of hemodialysis patients. J Atherosclerosis Thromb 2017; 24(4):412–421. doi:10.5551/jat.36426.
11. Kiraz K, Gökdeniz T, Kalaycıoglu E, et al. Epicardial fat thickness is associated with severity of disease in patients with chronic obstructive pulmonary disease. Eur Rev Med Pharmacol Sci 2016; 20(21):4508–4515.
12. Goeller M, Achenbach S, Marwan M, et al. Epicardial adipose tissue density and volume are related to subclinical atherosclerosis, inflammation and major adverse cardiac events in asymptomatic subjects. J Cardiovasc Comput Tomogr 2018; 12(1):67–73. doi:10.1016/j.jcct.2017.11.007.
13. Milanese G, Silva M, Bruno L, et al. Quantification of epicardial fat with cardiac CT angiography and association with cardiovascular risk factors in symptomatic patients: from the ALTER-BIO (Alternative Cardiovascular Bio-Imaging markers) registry. Diagn Interv Radiol 2019; 25(1):35–41. doi:10.5152/dir.2018.18037.

14. Nath J, Vacek JL, Heidenreich PA. A dilated inferior vena cava is a marker of poor survival. Am Heart J 2006; 151(3):730–735. 2006/03/01/ https://doi.org/10.1016/j.ahj.2005.04.023.
15. Miller JB, Sen A, Strote SR, et al. Inferior vena cava assessment in the bedside diagnosis of acute heart failure. Am J Emerg Med 2012; 30 (5):778–783. 2012/06/01/ https://doi.org/10.1016/j.ajem.2011.04.008.
16. Lippi G, Salvagno GL, Pegoraro M, et al. Assessment of immune response to SARS-CoV-2 with fully automated MAGLUMI 2019-nCoV IgG and IgM chemiluminescence immunoassays. Clin Chem Lab Med 2020. doi:10.1515/cclm-2020-0473.
17. Pan C, Chen L, Lu C, et al. Lung recruitability in COVID-19–associated acute respiratory distress syndrome: a single-center observational study. Am J Resp Crit Care Med 2020; 201(10):1294–1297.
18. Mahdavi A, Khalili N, Davarpanah AH, et al. Radiologic management of COVID-19: preliminary experience of the Iranian Society of Radiology COVID-19 Consultant Group (ISRCC). Iranian J Radiol 2020; 17(2): e102324doi:10.5812/iranjradiol.102324.
19. Miller J. Cardiac dimensions derived from helical CT: correlation with plain film radiography. Internet J Radiol 2000; 1(1).
20. Gollub MJ, Panu N, Delaney H, et al. Shall we report cardiomegaly at routine computed tomography of the chest? J Comput Assist Tomogr 2012; 36(1):67–71. doi:10.1097/RCT.0b013e318241e585.
21. Colombi D, Bodini FC, Petrini M, et al. Well-aerated lung on admitting chest CT to predict adverse outcome in COVID-19 pneumonia. Radiology 2020; 0(0):201433. doi:10.1148/radiol.2020201433.
22. Wynants L, Van Calster B, Bonten MMJ, et al. Prediction models for diagnosis and prognosis of covid-19 infection: systematic review and critical appraisal. BMJ 2020; 369:m1328. doi:10.1136/bmj.m1328.
23. Argulian E, Sud K, Vogel B, et al. Right ventricular dilation in hospitalized patients with COVID-19 infection. JACC Cardiovasc Imaging 2020. doi:10.1016/j.jcmg.2020.05.010.
24. Richardson S, Hirsch JS, Narasimhan M, et al. Presenting characteristics, comorbidities, and outcomes among 5700 patients hospitalized with COVID-19 in the New York City area. JAMA 2020; 323(20):2052–2059. doi:10.1001/jama.2020.6775. PubMed PMID: 32320003; PubMed Central PMCID: PMCPMC7177629 Regeneron outside the submitted work. Dr Becker reported serving on the scientific advisory board for Nihon Kohden and receiving grants from the National Institutes of Health, United Therapeutics, Philips, Zoll, and Patient-Centered Outcomes Research Institute outside the submitted work. Dr Cohen reported receiving personal fees from Infervision outside the submitted work. No other disclosures were reported. eng.
25. Iyer AS, Wells JM, Vishin S, et al. CT scan-measured pulmonary artery to aorta ratio and echocardiography for detecting pulmonary hypertension in severe COPD. Chest 2014; 145(4):824–832. doi:10.1378/chest.13-1422.
26. Spagnolo P, Cozzi A, Foà RA, et al. CT-derived pulmonary vascular metrics and clinical outcome in COVID-19 patients. Quant Imaging Med Surg 2020; 10(6):1325–1333. doi:10.21037/qims-20-546.
27. Madjid M, Safavi-Naeini P, Solomon SD, et al. Potential effects of coronaviruses on the cardiovascular system: a review. JAMA Cardiol 2020. doi:10.1001/jamacardio.2020.1286.
28. Zhou F, Yu T, Du R, et al. Clinical course and risk factors for mortality of adult inpatients with COVID-19 in Wuhan, China: a retrospective cohort study. Lancet 2020; 395(10229):1054–1062. doi:10.1016/s0140-6736 (20)30566-3. 2020/03//.
29. Guzik TJ, Mohiddin SA, Dimarco A, et al. COVID-19 and the cardiovascular system: implications for risk assessment, diagnosis, and treatment options. Cardiovasc Res 2020. doi:10.1093/cvr/cvaa106.
30. Vieillard-Baron A, Prin S, Chergui K, et al. Echo-Doppler demonstration of acute cor pulmonale at the bedside in the medical intensive care unit. Am J Respir Crit Care Med 2002; 166(10):1310–1319. doi:10.1164/rccm.200202-146CC.
31. Salehi S, Abedi A, Balakrishnan S, et al. Coronavirus disease 2019 (COVID-19): a systematic review of imaging findings in 919 patients. AJR Am J Roentgenol 2020: 1–7. doi:10.2214/ajr.20.23034.
32. Chung M, Bernheim A, Mei X, et al. CT imaging features of 2019 novel Coronavirus (2019-nCoV). Radiology 2020; 295(1):202–207. doi:10.1148/radiol.2020200230. 2020/04/01.
33. Qanadli SD, Beigelman-Aubry C, Rotzinger DC. Vascular changes detected with thoracic CT in Coronavirus disease (COVID-19) might be significant determinants for accurate diagnosis and optimal patient management. AJR Am J Roentgenol 2020. doi:10.2214/ajr.20.23185. 2020/04//:W1.

34. Dangis A, Gieraerts C, Bruecker YD, et al. Accuracy and reproducibility of low-dose submillisievert chest CT for the diagnosis of COVID-19. Radiol Cardiothorac Imaging 2020; 2(2):e200196doi:10.1148/ryct.2020200196.

35. Galiè N, Humbert M, Vachiery J-L, et al. ESC/ERS guidelines for the diagnosis and treatment of pulmonary hypertension: the joint task force for the diagnosis and treatment of pulmonary hypertension of the European Society of Cardiology (ESC) and the European Respiratory Society (ERS) endorsed by: Association for European Paediatric and Congenital Cardiology (AEPC), International Society for Heart and Lung Transplantation (ISHLT). Eur Resp J 2015; 46(4):903–975.

36. Coste F, Benlala I, Dournes G, et al. Assessing pulmonary hypertension in COPD. Is there a role for computed tomography? Int J Chron Obstruct Pulmon Dis 2019; 14:2065–2079. doi:10.2147/COPD.S207363.

37. Hoeper MM, Lee SH, Voswinckel R, et al. Complications of right heart catheterization procedures in patients with pulmonary hypertension in experienced centers. J Am Coll Cardiol 2006; 48(12):2546–2552. doi:10.1016/j.jacc.2006.07.061.

38. Winklhofer S, Berger N, Ruder T, et al. Cardiothoracic ratio in postmortem computed tomography: reliability and threshold for the diagnosis of cardiomegaly. 2014;10(1):44-49.

39. Hota P, Simpson S. Going beyond cardiomegaly: evaluation of cardiac chamber enlargement at non−electrocardiographically gated multidetector CT: current techniques, limitations, and clinical implications. 2019; 1(1):e180024.doi:10.1002/bjs.18002610104.

40. Skulstad H, Cosyns B, Popescu BA, et al. COVID-19 pandemic and cardiac imaging: EACVI recommendations on precautions, indications, prioritization, and protection for patients and healthcare personnel. Eur Heart J Cardiovasc Imaging 2020; 21(6):592–598. doi:10.1093/ehjci/jeaa072.